Journal of Engineering Science and Technology
Vol. 15, No. 5 (2020) 3388 - 3403


# SURFACE ROUGHNESS ASSESSMENT BASED ON DIGITAL IMAGE TEXTURE ANALYSIS OF CFRP COMPOSITES MACHINED BY SWIRLING ABRASIVES

S. MADHU[1], M. BALASUBRAMANIAN[2,*], S. KANNAN[3]

[1]Saveetha School of Engineering, 602105, India
[2]R.M.K College of Engineering and Technology, 601206, India
[3]Hindusthan College of Engineering and Technology, India
*Corresponding Author: manianmb@gmail.com

## Abstract

Due to the heterogeneity properties of composite materials, the mechanism of material removal is the aspect of divergence between metallic materials and composites. Mechanical failure, nonconformity in the tolerance and roughness of the hole surface using conventional drilling process caused the component to be rejected in the manufacturing industries. In this experimental work carbon fiber polymeric composite material was used as work piece and holes were made using abrasive jet machining (AJM) with 3 start internal threaded nozzle. Average surface roughness (Ra) was measured by conventional stylus instrument. The traditional surface roughness measuring instruments are sensitive and they penetrate or scratch the material surface. To avoid the unwanted damage on the work piece surface, optical measuring systems were used. In this research a new method of image processing-based surface roughness detection technique is proposed in this work. A charged coupled device (CCD) camera was used for scanning the grayscale images of abrasive jet machined hole. Based on the histograms from the optical objects of machined Carbon fiber reinforced polymer composites (CFRP) hole image surface roughness parameters were derived. A statistical method using CLCM was used for examining the AJM hole texture and the CFRP hole surface roughness was measured. Image through histogram-based segmentation and contrast method were analyzed and evaluated through pixel distance calculation method. In this research minimum surface roughness (Ra) measured by stylus was 0.315 µm and Ra was computed from the magnified surface texture image was 0.327. Percentage of error is -3.81. Surface roughness measured from the stylus technique was compared with the estimated values. Surface roughness measured from the stylus technique was compared with the estimated values.

Keywords: AJM, CFRP, Image processing, Surface roughness, Threaded nozzle.

## 1. Introduction

In automobile industries global warming and fuel usage has led to growing demand for light weight components and structures. To fulfil the demand, carbon fibre composites (CRFP) composites were widely used. Hole making using drilling process in CRFP may result in delamination of the layers and several other defects like dimensional defects, surface roughness and surface integrity. Nearly 60 % of all components that is discarded is because of poor quality of the hole [1]. In general, polymer composites are produced to near to net shape. During drilling, the work surface may get damaged resulting in aesthetic issues and the risk of mechanical failures increase substantially [2]. Hence unconventional machining method is preferable to machine the composites. AJM is one of the established machining methods to drill the composites.

Surface roughness is the important factor of all manufactured. Because of the non-homogenous property, reliable surface roughness measurement of fibre reinforced polymer composites was challenging. Surface roughness (Ra) is measured using stylus type instrument with high consistency. The tip of the instrument could not reach into all the surface valleys thus filter of surface data is low. Due to the tip radius, the measurement of fine surfaces has limitation.

Information about the image collected using camera is processed by greyscale equalization and histogram conversion amplification. Normalized cross-correlation and surface fitting techniques were used to analyse the data. Arithmetic surface roughness measured by using portable surface roughness apparatus (TR240) [3]. As a result of combinations of parameters, various surface characteristics and properties were produced [4]. Captured images in the database were used as reference to predict surface roughness using Euclidean and hamming distances. The surface roughness measured using stylus instrument was characterized by MATLAB Image processing to evolve a vision based image processing techniques [5]. MATLAB software was used for characterizing the machined surface images for roughness estimation [6]. Speckle correlation technique was used for estimating the milled and ground surfaces. These patterns were captured using charged couple device (CCD) with collimated laser beam. It was noticed that the surface roughness (Ra) obtained using stylus instrument correlated with the predicted Ra [7]. Different fibre (glass, jute, vika, hemp, and banana) reinforced polymer composites were machined using the process of milling.

Roughness (Ra) obtained from both conventional (Talysurf stylus instrument) and image processing (co-efficient of variance) based techniques was analysed. It was observed that the image processing parameters depends upon the colour of the surface texture [8]. Computer vision technique was used for capturing the surface roughness peaks. C++ software was used for translating the colour texture images into grey scale images and stores as 2 dimensional array matrixes. Surface roughness (Ra) measured using Talysurf instrument correlated with the standard sine wave produced by image processing software [9]. Images captured were converted into binary images for evaluating the surface roughness using MATLAB software. It is observed that the direction of the black and white lines significantly affects the estimated surface roughness [10].

Horning process was performed on cylinder bore made up of grey cast were characterized by image based curve parameter (Abbott-Firestone). It was noticed that the estimated image processing results correlated between measured the

surface roughness of the cylinder bore accurately [11]. Surface texture evaluation method of castings specimens with irregular texture with 2 surface roughness values Ra (6.3, 25, 50) and Rz (6.3, 12.5, 25, 50) were evaluated using k-means morphology image segmentation method [12]. The quality of drilled hole in GFRP was investigated by Image J, fuzzy logic model. It was concluded that the results from digital image processing, regression model and Fuzzy output prediction were in good correlation [13]. Roughness parameters of metal parts were investigated using covariance functions and wavelet's wave method. In this investigation the surface roughness of the metal parts was estimated using RGB colour spectrum [14]. Polynomial based network image processing system was developed for measuring the surface roughness of C55 steel using turning process under different process parameters. Maximum error between the measured and estimated surface roughness obtained was less than 11.32% [15]. Surface roughness (Ra) obtained from the conventional measuring method has been compared with texture features of the machined surfaces formed by wavelet transformation [16].

A non-contact method of pattern classifier image processing method was used to measure the surface roughness (Ra and Rz) [17]. Super resolution reconstruction algorithm for pre-processing the digital images has been used to predict the surface roughness. The predicted surface roughness shows better correlation with the roughness obtained from the contact type stylus measurement method. It was also noticed that super resolution reconstruction algorithm was used for estimating the surface roughness based on the digital images [18]. Online machine vision method was developed for estimating the surface roughness (Ra) of machined steel work piece surface using feed forward multi-layer perception artificial neural. The machined surface roughness image was captured and transformed using Fourier transform algorithm. The surface roughness predicted by artificial neural network was found to be in close agreement with the measured optical roughness [19]. Handy surf E-10 roughness instrument was used for measuring the roughness. Grey level co concurrence matrix (GLCM) was used for this investigation [20]. The calculation of Ga, optical roughness value, after applying geometric search technique had a better correlation with the average surface roughness (Ra) [21].

Roughness parameters can be assessed using the characteristics extracted from the images without the need of machining parameters [22]. Images captured were exported from VG Studio Max 2.2 for estimating the diameter, circularity and delamination [23]. Surface roughness of the samples machined by conventional method and image analysis resulted in the correlation coefficient between 0.8 and 1 [24].

Experimental characterization was conducted in polymer based unidirectional carbon fiber reinforced composite laminate by using non-contact digital image correlation technique and compared [25]. Face milled aluminium 6060 work piece digital images for generating the fuzzy inference system to estimate the surface roughness (Ra) using the adaptive neuro fuzzy method. It was seen that the error obtained between measured and estimated is 6.98 % [26]. The work piece images acquired using a digital camera and polynomial network based self-organizing adaptive method was applied to measure the surface roughness. The roughness obtained from the turned steel bar surface was estimated with realistic precision [27]. Laser beam detection method based on image processing technique and image recognition algorithm was proposed to estimate the roughness (Ra) of the tiles. This investigation concluded that roughness less than 0.35 mm over an area of 60 ×60 cm can be recognized effectively [28].

Previous research researchers investigated the effect of abrasive water jet parameters on average surface roughness in carbon fibre reinforced polymer composites. The author's previous work investigated the influence of mixture of air and abrasive particles flow through the nozzle on surface roughness (Ra). In this work, 3 start internal threaded nozzles were used for making whirling effect on air and abrasive particle mixture [29].

Carbon fibre composites machined using AWJ. This work reported that, maximum pressure resulted in better peeling of the carbon fibers from the matrix. Also for the maximum pressure the lower kinetic energy of the water jet resulted in poor cutting efficiency which in turn increased the average surface roughness [30]. Abrasive water jet machining experiments conducted on carbon fibre composites. This work reported that stand-off distance was the significant parameter which reduced the surface roughness and the minimum of 1.53 µm surface roughness was obtained [31]. Garnet abrasive particles was used for machining prepreg laminates reinforced with carbon fiber using the epoxy polymer resin matrix ($120 \times 150 \times 5$ $mm^3$ ) using abrasive water jet. It was noted garnet particles with maximum pressure reduced the surface roughness of the CFRP samples [32]. Abrasive water jet drilling processes have been employed to produce holes on 3 mm woven CFRP sheets. It was seen that holes top diameter is greater than the bottom also the hole diameter and wall inclination angle increase with an increase in SOD. Hole defects, such as surface chipping, edge damage, delamination, and internal cracking, have been found if the process parameters are not selected properly [33].

Based on the findings from the previous works discussed with respect to abrasive jet machining of CFRP composites, achievement of the swirling jet possible as the nozzle is made of a single part and the threads are inside the nozzle surface. In this current investigation a non-contact method was used for measuring Euclidean distance and hamming distance of the reference images. In this work CCD camera was used for scanning the grayscale images of abrasive jet machined hole. Stylus instrument was used for measuring the roughness of reference surfaces and stored in the database. A statistical method using CLCM was used for examining the AJM hole texture and the CFRP hole surface roughness was measured. Image through histogram-based segmentation and contrast method were analyzed and evaluated through pixel distance calculation method. From the optical abrasive jet machined hole image, surface roughness (Ra) were derived based on the histograms. Thus, the average surface roughness (Ra) is estimated and the reference image can be endorsed with test image. Online and non-contact measurement of average roughness (Ra) in carbon fibre reinforced polymer (CFRP) composite is scanty.

In the present study, holes were made on CFRP composite using an abrasive jet machining (AJM) with internal threaded nozzle. Surface roughness (Ra) across the hole was measured using stylus type instrument. The machined surface images were captured and feed in to the image processing software and predicted surface roughness from the digital images.

## 2. Materials and Methods

### 2.1. Material

Reinforcements (carbon fibers) act as load bearing element, whereas the matrix (epoxy resin) encloses the fibers and protects them in the desired direction.

Matrices act as load transfer elements between the fibers and protect the structure against harsh environmental conditions such as high temperature and humidity [34, 35]. In this current research carbon fibre with 1.75 g/cm$^3$ density reinforced with 1.10 g/cm$^3$ of epoxy resin. The weigh percentage of carbon fibre is 42.81 and epoxy resin is 57.19 respectively used and using hand layup process 300 x 300 mm carbon fiber reinforced polymer composites were fabricated and used as work pieces for this investigation. The samples were cut to the required dimension for experimentation. The size of each specimen cut from the cast sheet is 50 x 15 x 5 mm [32]. 31 samples were prepared and used as the work piece for abrasive jet machining (AJM).

## 2.2. Experimental technique

The abrasive jet nozzles with internal threads were fabricated in five different diameters (1.5, 2, 2.5, 3, and 3.5 mm) as per the dimensions. The internal threaded nozzles are made up of hardened steel. Figure 1 shows the cut section of the threaded nozzles. The key factors (pressure, stand-off distance, nozzle diameter and abrasive size) having influence on surface roughness (Ra) have been recognized on the basis of the investigational work done previously.

Aluminum oxide ($Al_2O_3$), silicon carbide (SiC), sodium bicarbonate ($NaHCO_3$), and glass beads are commonly used abrasives in abrasive jet machining. Abrasive particles are usually selected on the basis of application**.** Alumina is used for cleaning, cutting and deburring purposes for moderate to hard materials. SiC is harder abrasive compared to alumina. Thus can be used for all the above purposed but for very hard and tough materials. In this current research the work piece selected is carbon fibre reinforced composites with 5 mm thickness. Since CFRP is a hard and tough fibre reinforced composites, SiC abrasives with dissimilar sizes were blown through the fixed nozzle. Carbon fibre reinforced epoxy laminates were employed for experimentation as per the condition mentioned in Table 1.

**Table 1. Abrasive jet machining conditions.**

| | |
|---|---|
| **Machine Setup** | Vortex-type mixing Chamber |
| **Abrasives** | Silicon carbide |
| **Medium** | Air |
| **Nozzle Material** | Hardened steel, threaded |
| **Operating Angle** | $90^0$ |
| **Work piece Material** | Carbon Fiber Reinforced Polymer Composite |

In the earlier studies, abrasive jet process parameters chosen for machining of composite materials are jet pressure, stand-off distance, abrasive flow rate, mixing ratio, abrasive grain size, type of abrasive particle, nozzle diameter, jet impingement angle. But predominantly the factors such as pressure, stand-off distance, nozzle diameter and abrasive size were considered to be the important factors [36, 37]. Review of literature and the trial works done in the author's laboratory have helped identifying the predominant abrasive jet factors which have greater influence on surface roughness (Ra).The predominant factors are presented below (i) Pressure (*P*)(ii) Stand-off distance (*SOD*) (iii) Nozzle diameter (*D*) (iv) Abrasive size (*S*).

When the pressure was below 0.2 MPa the particle velocity was not sufficient to reach the bottom surface of the work piece causing the uncut region at the bottom surface and when the pressure was above 0.6 MPa the abrasive particles impinging the work piece resulted in rough machined surface. When the SOD is below 0.5 mm, large amount of abrasive particles logged in to the 0nozzle tip and could not effectively machine the work surface and when the SOD is above 2.5 mm the jet divergence is more causing, poor machining. When the nozzle diameter is below 1.5 mm, the jet impingement area is less and when the nozzle diameter is above 3.5 mm the kinetic energy of the jet is decreased. Also it is much difficult to make internal threads inside the nozzle when the diameter was below 1.5 mm. When the abrasive particle size is below 50 micron, the material removal rate was minimized and when the particle size is above 130 micron the surface roughness reduced. Hence some uncut regions were seen in the top and bottom surface of the work piece. Based on the above investigations, the range of factors for experimentation were decided and presented in the Table 2.

**Table 2. Important factors and their working range.**

| Factor | Notation | Unit | Levels | | | | |
|---|---|---|---|---|---|---|---|
| | | | (-2) | (-1) | (0) | (+1) | (+2) |
| **Pressure** | *P* | MPa | 0.2 | 0.3 | 0.4 | 0.5 | 0.6 |
| **SOD** | *L* | mm | 0.5 | 1 | 1.5 | 2 | 2.5 |
| **Nozzle diameter** | *D* | mm | 1.5 | 2 | 2.5 | 3 | 3.5 |
| **Abrasive size** | *S* | microns | 50 | 70 | 90 | 110 | 130 |

A total of 31 holes were made on CFRP samples according to a $2^4$ full factorial design. Roughness (Ra) across the hole was measured using surf test (SJ-210 series) surface roughness instrument with the specification of range: 17.5 mm; speed: 0.25, 0.5, and 0.75 mm/s; tip radius: 5 µm; detector angle: 90º. To prevent the error and better precision Ra was accomplished directly on the machined hole surface at three different locations and were repeated three times.

**Fig. 1. Cut sectional view of internally threaded nozzle.**

## 2.3. Image processing

Optical microscope (DE-WINTER inverted Trinocular) equipped with digital camera configured for 95 X magnification was used for capturing eight-bit TIFF

images at a resolution of 2087 pixels per mm. In the corresponding topography, light areas are shown as mountains and the dark areas as valleys. In this work surface roughness (Ra) was computed from the magnified surface texture image. Figure 2 shows the abrasive jet machined images captured using optical microscope. The CCD vision system was used for scanning the grey scale images from an area of the machined CFRP work piece. Based on the histograms of machined surface new optical roughness parameters were derived. Surface roughness parameters are measured based on GLCM method. In this work histogram-based segmentation and contrast method were implemented. The material roughness evaluated through pixel distance calculation of two points in image and analyzes the result in micron based conversion. Figure 3 shows the process of measuring surface roughness using Mat lab.

**(a) Top hole** **(b) Bottom hole**

**Fig. 2. Optical macro images of AJM hole.**

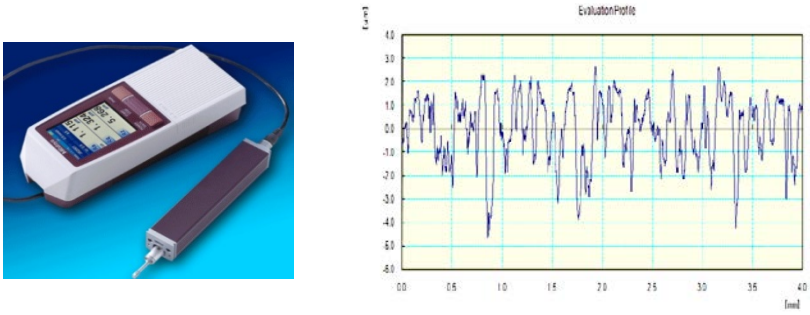

**Fig. 3. Surface roughness (Ra) measuring method.**

## 2.4. AIN binarization

The Phase Rotation Congruency Covariance (PRCC) is the scheme used here which performs pixels degree rotation in both horizontal and vertical direction to select the better pixel angle to improve the pixel quality. Then the reconstruction process involves dense retrieval of an image. Here the process includes reconstructing of an image in a dense form after the PRCC is performed. If image intensity is less than T, thresholding method replaces each image with a black pixel [20]. As a result, the dark becoming black and the white snow becomes white as shown in Fig. 4.

**Fig. 4. Threshold image.**

## 2.5. Grey level co-occurrence matrix (GLCM)

GLCM is a 2 dimensional matrixes constructed by counting the number of occurrences of pixel pairs as specified by a position operator. Grey level co-occurrence matrix planned for symmetric and non-symmetric matrices. For non-symmetric matrices, eight PPD could be used to calculate the matrices [26]. The following algorithm is used for calculating the GLCM for the roughness of CFRP work pieces. It is used for the different position of operators. It represents a matrix which contains an image size of 7×7 with six grey levels (0-5) as shown in Fig. 5. A position operator P1, 0; is used to calculate GLCM which produces a non-symmetric matrix and P1, (180 + 0) produces symmetric matrix which can be shown in Fig. 5. The black cells indicate the main diagonal of the matrix [14, 15].

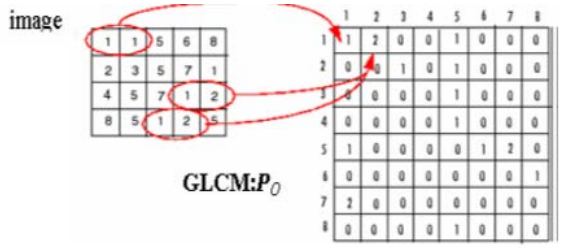


**Fig. 5. Symmetric matrix.**

## 2.6. Algorithm

The Grey Level Co-occurrence Matrix (GLCM) is constructed from the image by estimating the pair wise statistics of pixel intensity. Each element of the matrix represents an estimate of the probability that two pixels with a specified separation have grey levels. The separation is usually specified by a displacement, and an angle. In our study, Contrast, Correlation, Energy and Homogeneity are considered. The GLCM features are calculated for abrasive jet machined holes at various process parameters [16].

```
R = sum (sum (GLCM))
Norm_GLCM_region = GLCM/R;
Ent_int = 0;
For k = 1: length (GLCM) ^2
IfNorm_GLCM_region (k) ~=0
Ent_int = Ent_int + Norm_GLCM_region (k)*log2 (Norm_GLCM_region (k));
End
End.
```

## 3. Results and Discussion

By using GLCM process in image processing various feature of the image can be determined by using Euclidean pixel distance measurement point to point roughness can be calculated. Table 3 shows the analysed values of the image processing. The measurements considered for the threaded surface images are shown in Figs. 6(a)-(h). This helps to identify the difference in surface roughness detection. The percentage of error was calculated using the following formula [27].

% of Error = 100×(Actual Ra - Estimated Ra)/Actual Ra/

**Table 3. Feature extraction from GLCM for hole images made by threaded nozzle.**

| Image | Contrast | Correlation | Energy | Homogeneity |
|---|---|---|---|---|
| Image 01 | 363.3123 | 0.9077 | 0.0036 | 0.2581 |
| Image 02 | 715.8936 | 0.7962 | 6.0082e-004 | 0.1525 |
| Image 03 | 381.5672 | 0.9175 | 1.3094e-004 | 0.1569 |
| Image 04 | 1.1026e+003 | 0.6404 | 9.2360e-005 | 0.1024 |
| Image 05 | 381.4047 | 0.9175 | 1.3096e-004 | 0.1568 |
| Image 06 | 729.0768 | 0.8723 | 2.8469e-004 | 0.1431 |
| Image 07 | 908.0654 | 0.7706 | 3.5053e-004 | 0.1359 |
| Image 08 | 719.0412 | 0.8112 | 2.7467e-004 | 0.1211 |

### 3.1. Influence of AJM machining parameters on measured and estimated roughness (Ra).

Table 4 shows the relationship between the measured and estimated roughness of carbon fibre composites samples used for this investigation. The investigation indicates the minimum surface roughness obtained from the threaded nozzle is 0.315 µm. Figure 6 indicates the outcome of abrasive jet machining parameters on surface roughness (Ra).

**Table 4. Comparison between the measured and estimated surface roughness CFRP samples.**

| | Abrasive jet parameter | | | | Surface roughness (µm) | | |
|---|---|---|---|---|---|---|---|
| Selected samples | Pressure (bar) | Stand-off distance (mm) | Nozzle dia (mm) | Abrasive size (micron) | Measured by stylus | Estimated by image processing | Percentage of error |
| Image 01 | 2 | 1.5 | 2.5 | 90 | 0.669 | 0.712 | -6.43 |
| Image 02 | 6 | 1.5 | 2.5 | 90 | 0.315 | 0.327 | -3.81 |
| Image 03 | 4 | 0.5 | 2.5 | 90 | 0.469 | 0.423 | 9.81 |
| Image 04 | 4 | 2.5 | 2.5 | 90 | 0.618 | 0.606 | 1.94 |
| Image 05 | 4 | 1.5 | 1.5 | 90 | 0.622 | 0.675 | -8.52 |
| Image 06 | 4 | 1.5 | 3.5 | 90 | 0.722 | 0.767 | -6.23 |
| Image 07 | 4 | 1.5 | 2.5 | 50 | 0.372 | 0.366 | 1.61 |
| Image 08 | 4 | 1.5 | 2.5 | 130 | 0.509 | 0.487 | 4.32 |

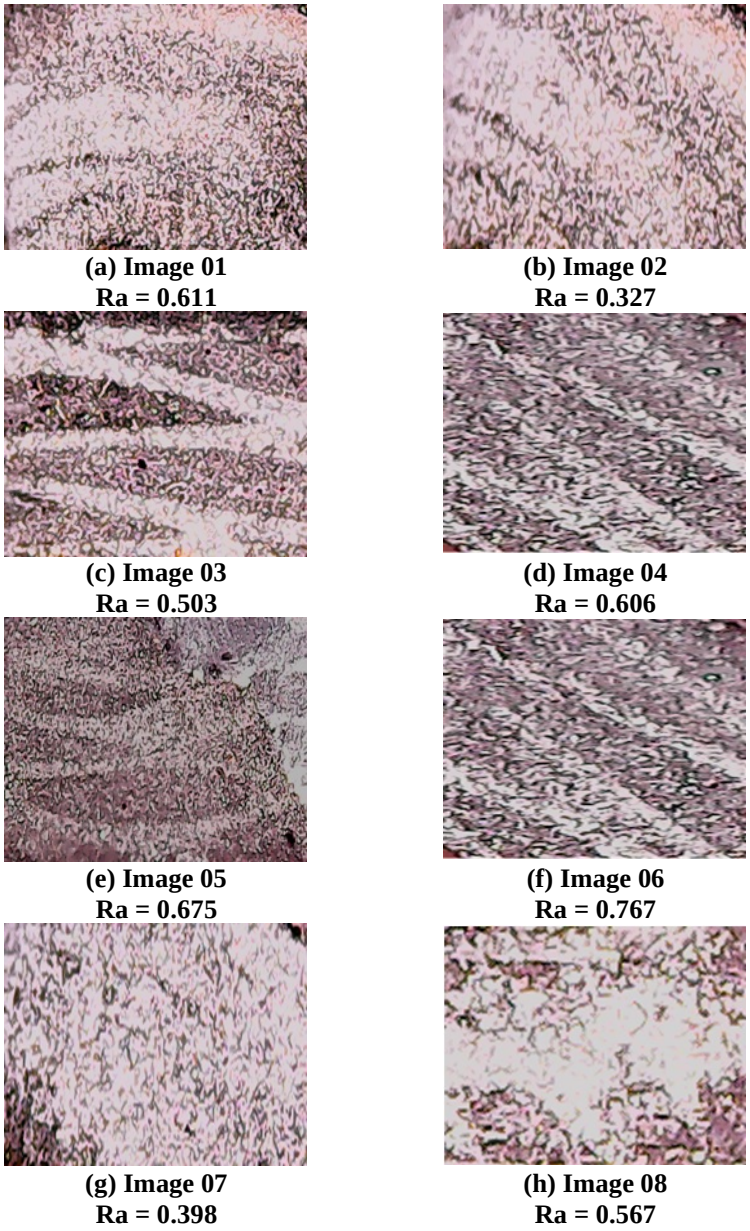

**(a) Image 01**
**Ra = 0.611**

**(b) Image 02**
**Ra = 0.327**

**(c) Image 03**
**Ra = 0.503**

**(d) Image 04**
**Ra = 0.606**

**(e) Image 05**
**Ra = 0.675**

**(f) Image 06**
**Ra = 0.767**

**(g) Image 07**
**Ra = 0.398**

**(h) Image 08**
**Ra = 0.567**

**Fig. 6. Sample images with estimated surface roughness by image processing.**

## 3.2. Influence of pressure (*P*)

When the pressure is maximum (0.6 MPa), the surface roughness (Ra) obtained using threaded nozzle was 0.315 μm and estimated surface roughness from image processing was 0.327 μm. The percentage of error is 3.81. When the jet pressure is minimum (0.2 MPa), the CFRP hole surface roughness obtained from the internal threaded nozzle is 0.669 μm and the estimated surface roughness from image processing was 0.712 μm. The percentage of error is 6.41. From this

investigation, at a maximum pressure level, internal threaded nozzle reduced the surface roughness. The effect of pressure on the surface on measured and estimated surface roughness (Ra) is shown in Fig. 7(a). As the abrasive jet pressure increases, the abrasive particles are cut down into smaller sizes. Further, the threaded profile inside the nozzle surface causes whirling of the particles inside the nozzle while the kinetic energy is increased, increasing the smoothness of the work piece surface [18,21].

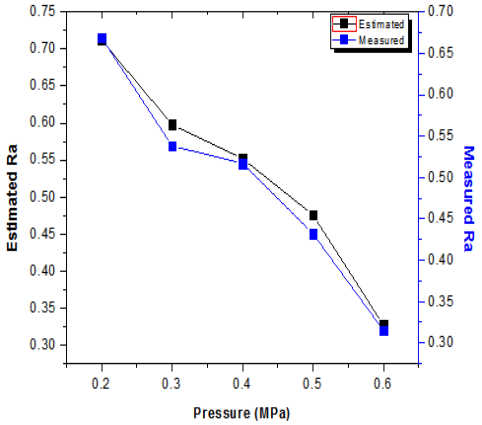


**(a) Effect of pressure on surface roughness (Ra)**

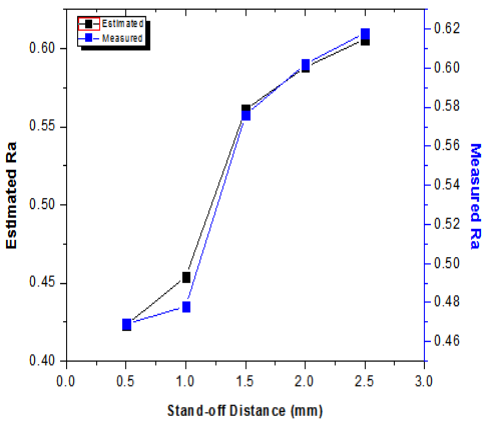


**(b) Effect of SOD on surface roughness (Ra)**

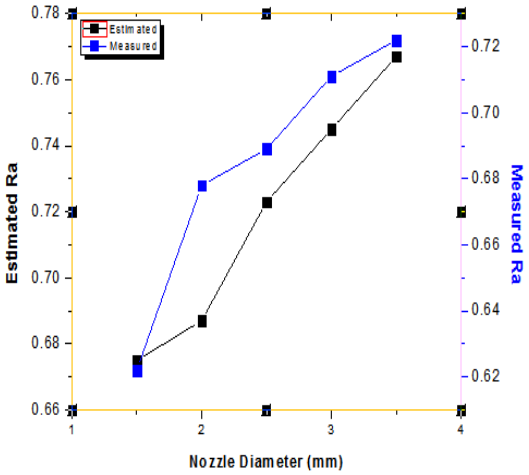


**( c ) Nozzle diameter vs. surface roughness (Ra)**

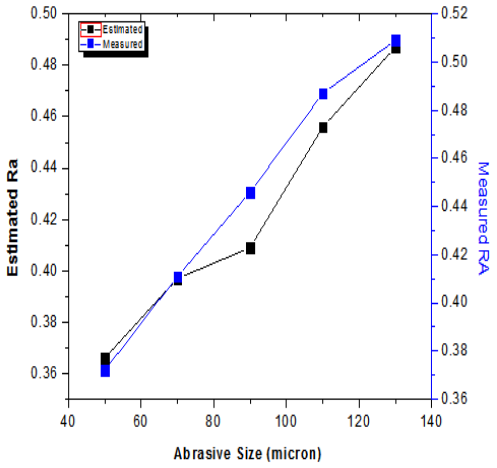


**(d) Abrasive size vs. surface roughness (Ra)**

**Fig. 7. Effect of abrasive jet parameters on surface roughness.**

As the abrasive jet pressure increased, the cutting process enabled without severe jet deflection which in turn minimize the waviness pattern. As a result, the surface roughness decreased. Further, the threaded profile of the nozzle caused

whirling of the particles inside the nozzle and when the kinetic energy was increased, decreasing the surface roughness of the CFRP composite [32].

### 3.3. `Influence of stand-off distance (*L*)

When the distance between the threaded nozzle tip and the carbon fibre work piece is lowest, the roughness (Ra) obtained is 0.469 μm and the estimated surface roughness from image processing was 0.423 μm. The percentage of error is 9.81. As a result of higher stand-off distance, threaded nozzle offer 0.618 μm surface roughness and the estimated surface roughness from image processing was 0.606 μm. In this current investigation, percentage of error obtained is 1.94. Figure 7(b) shows the effect of SOD on measured and estimated roughness (Ra) of carbon fibre composite machined by AJM. As the stand-off distance increases, the diameter of the jet also increases [29]. So the kinetic energy decreases before the jet reaches the work surface. Hence, surface roughness (Ra) increased with the increase in stand-off distance (SOD). Higher SOD allows the jet expands before impingement which may increase vulnerability to external drag from the surrounding environment. So the kinetic energy got decreased before the jet reached the work surface. The cutting ability of particle reduces and hence, surface roughness increased with increase in stand-off distance [33].

### 3.4. Influence of nozzle diameter (*D*)

The surface roughness (Ra) obtained from the threaded nozzle for 1.5 mm diameter is 0.622 μm and the estimated roughness from image processing is 0.675 μm. The percentage of error is 8.52. With the higher nozzle diameter (3.5 mm), the measured roughness is 0.722 μm and the estimated roughness from image processing is 0.767 μm. The percentage of error is 6.23. Figure 7(c) indicated the effect of nozzle diameter on measured and estimated surface roughness (Ra) of CFRP samples. When the mixture of air and abrasive particle jet coming out from larger diameter internal threaded nozzle, the SiC particles lose their kinetic energy before impinging the carbon fibre composite work pieces. The threads presented inside the nozzle causes particle flow of in a whirling action. It makes the particles gain high kinetic energy [21]. When a mixture of air and abrasive particle flows from the nozzle with a larger diameter, the particles may lose their kinetic energy. The presence of an internal thread inside the nozzle causes particle flow in a whirling motion. It helps the particles to gain a high kinetic energy. Further smaller nozzle diameter increases the flow rate. This causes a smaller diameter nozzle with internal threads reduced the surface roughness [34].

### 3.5. Influence of abrasive size (*S*)

The SiC abrasives with 130 micron coming out from the threaded nozzle offered surface roughness of 0.509 μm and the estimated roughness from image processing is 0.487 μm. The percentage of error is 4.32. The abrasive particle with smaller mesh size of 50 micron gives a surface roughness (Ra) of 0.372 μm and the estimated roughness from image processing is 0.366 μm. From the current investigation, percentage of error obtained is 1.61. Figure 7(d) mentioned the influence of abrasive particle size on measured and estimated surface roughness (Ra). In the threaded nozzle, maximum size of abrasive particles got whirl, and increase the particle velocity caused decrease the surface roughness (Ra) of CFRP

composites. Hence, the minimum abrasive particle size flowing through the nozzle reduced the surface roughness [36]. The surface roughness obtained was minimum in threaded nozzle when compared with unthreaded nozzle. The smaller abrasive particle reached the bottom hole surface without losing the kinetic energy. So, the minimum abrasive particle size flow through the nozzle caused a reduction in the surface roughness. The surface roughness is minimum in internal threaded nozzle as compared with the unthreaded nozzle [37].

It can be seen from this work assessing the roughness of abrasive jet machined hole on the basis of the features of digital image that the range of measured roughness has a great impact on the level of error assessing. The wider the range of measured roughness, with the uniform distribution by the roughness classes, the lower the error of assessment. The error of assessment in this study (5.33 %) was significantly influenced by process parameters. Without outliers the error of assessment of the machined surface roughness is expected to be significantly lower. In future, Aluminium (6061-T6), Titanium (Ti-6Al-4V), and Stainless steel (316L) will machined with the newly designed novel internal threaded nozzle to understand the effect of the process parameters on surface roughness.

## 4. Conclusions

In this work, an image processing algorithm was used for measuring the average surface roughness (Ra) of CFRP composites machined by abrasive jet machine using internal threaded nozzle. An enhanced method based on microscopic vision was used for detecting the Ra. Estimation model of Ra is employed by GLCM.

- Based on the experiments it was concluded that maximum jet pressure (6 bar) reduced the surface roughness as 0.315 μm and the estimated from image processing is 0.327 μm.
- When the pressure increased, the jet velocity increased which in turn increased the kinetic energy of the abrasive particle impinged the CFRP surface caused increased the cutting ability. Hence the surface roughness reduced. During abrasive jet machining, SiC abrasive particles break down into smaller pieces when flowed through the threaded nozzle.
- Moreover, when pressure increases, kinetic energy of the particles also increased. More kinetic energy removes maximum amount of material providing a smooth finish and thus reducing the roughness value.

### Nomenclatures

| | |
|---|---|
| *D* | Nozzle diameter, mm |
| *L* | Standoff distance, mm |
| *P* | Pressure, MPa |
| *Ra* | Surface roughness, micrometre |
| *S* | Abrasive size, microns |

**Abbreviations**

| | |
|---|---|
| AJM | Abrasive Jet Machining |
| CCD | Charged Coupled Device |
| CFRP | Carbon Fibre Reinforced Polymer |

| | |
|---|---|
| CLCM | Color Level Co-Occurrence |
| GFRP | Glass Fibre Reinforced Polymer |
| GLCM | Grey Level Co-Occurrence Matrix |
| PRCC | Phase Rotation Congruency Covariance |
| SiC | Silicon Carbide |
| SOD | Stand Off Distance |

## References


1. Liu, D.; Tang, Y.; and Cong, W.L. (2012). A review of mechanical drilling for composite laminates. *Composite Structures*, 94, 1265-1279.
2. Ramulu, M.; Wern, C.W.; and Garbini, J.L. (1993). Effect of fibre direction on surface roughness measurements of machined graphite/epoxy composite. *Composite Manufacturing*, 4, 39-51.
3. Zhongxiang, H.; Lei, Z.; Jiaxu, T.; Xuehong, M.; and Xiaojun, S. (2009). Evaluation of three-dimensional surface roughness parameters based on digital image processing. *International Journal of Advanced Manufacturing Technology*, 40, 342-348.
4. Gadelmawla, E.S.; Koura, M.M.; Maksoud, T.M.A.; Elewa, I.M.; and Soliman, H.H. (2002). Roughness parameters. *Journal of Materials and Processing Technology*, 123, 133-145.
5. Jeyapoovan, T.; and Murugan, M. (2013). Surface roughness classification using image processing. *Measurement*, 46, 2065-2072.
6. Srivani, M.; and Anthony Xavior, M. (2014).Investigation of surface texture using image processing techniques. *Procedia Engineering*, 97, 1943-1947.
7. Dhanasekar, B.; Krishna Mohan, N.; Basanta Bhaduri.; and Ramamoorthy, B. (2008). Evaluation of surface roughness based on monochromatic speckle correlation using image processing. *Precision Engineering*, 32, 196-206.
8. DilliBabu, G.; Sivaji Babu, K.; and Uma Maheswar Gowd, B. (2014). Evaluation of surface roughness of machined fiber reinforced composites plastics using image processing. *Applied Mechanics and Materials*, 573, 627-631.
9. Gadelmawla, E.S.; Koura, M.M.; Maksoud, T.M.A.; Elewa, I.M.; and Soliman, H.H. (2001). Estimation of surface roughness for turning operations using image texture features. Proceedings of the Institution of Mechanical Engineers. *Part B: Journal of Engineering Manufacture*, 225, 1281-1292.
10. Samtaş, G. (2014). Measurement and evaluation of surface roughness based on optic system using image processing and artificial neural network. *International Journal of Advanced Manufacturing Technology*, 73, 353-364.
11. Lawrence, K.D.; Shanmugamani, R.; and Ramamoorthy, B. (2014). Evaluation of image based Abbott–Firestone curve parameters using machine vision for the characterization of cylinder liner surface topography. *Measurement*, 55, 318-334.
12. Yang, M.; Zhang, X.; Liang, C.; and Liao, Q. (2011) Evaluating surface roughness of castings using K-means clustering and watershed transform. *IEEE International Conference on Multimedia Technology*, Hangzhou, China, 6345-6348.

13. Ragothaman, P.; and Unnikrishnan, A. (2014). Delamination analysis in drilling of composite materials using digital image processing, regression modelling and fuzzy logic. *International Journal of Mechanical and Production Engineering*, 2, 26-30.
14. Jurevicius, M.; Skeivalas, J.; and Urbanavicius, R. (2014). Analysis of surface roughness parameters digital image identification. *Measurement*, 56, 81-87.
15. Lee, B.Y.; Juan, H.; and Yu, S.F. (2002). A study of computer vision for measuring surface roughness in the turning process. *International Journal of Advanced Manufacturing Technology*, 19(4), 295-301.
16. Morala-Argüello, P.; Barreiro, J.; and Alegre, E. (2012). A evaluation of surface roughness classes by computer vision using wavelet transform in the frequency domain. *The International Journal of Advanced Manufacturing Technology*, 59 (1-4), 213-220.
17. Akbari, A.A.; Fard, A.M.; and Chegini, A.G. (2006). An effective image based surface roughness estimation approach using neural network. *Proceedings of World Automation Congress*, Budapest, Hungary.
18. Dhanasekar, B.; and Ramamoorthy, B. (2008). Assessment of surface roughness based on super resolution reconstruction algorithm. *International Journal of Advanced Manufacturing Technology*, 35(11-12), 1191-1205.
19. Fadare, D.A.; and Oni, A.O. (2009). Development and application of a machine vision system for measurement of surface roughness. A*RPN Journal of Engineering and Applied Sciences*, 4, 5, 30-37.
20. S Gadelmawla, E.; A Al-Mufadi, F.; and S Al-Aboodi, A. (2013).Calculation of the machining time of cutting tools from captured images of machined parts using image texture features. *Proceeding of the Institution of Mechanical Engineer Part B: Journal of Engineering Manufacture*, 225, 203-214.
21. Nithyanantham, N.; and Suresh, P. (2016). Evaluation of cast iron surface roughness using image processing and machine vision system. *ARPN Journal of Engineering and Applied Sciences*, 11 (2), 1111-1116.
22. Kamguem, R.; Tahan, S.A.; and Songmene, V. (2013). Evaluation of machined part surface roughness using image texture gradient factor. *International Journal of Precision Engineering and Manufacturing*, 14(2), 183-190.
23. Kourra, N.; Warnett, J.M.; Attridge, A.; Kiraci, E.; Gupta, A.; Barnes, S.; and Williams, M.A. (2015). Metrological study of CFRP drilled holes with x-ray computed tomography. *International Journal of Advanced. Manufacturing Technology*, 78 (9-12), 2025-2035.
24. Valíček, J.; Držík, M.; Hryniewicz, T.; Harničárová, M.; Rokosz, K.; Kušnerová, M.; Barčová, K.; and Bražina, D. (2012).Non-contact method for surface roughness measurement after machining. *Measurement Science Review*, 12 (5), 184-188.
25. Kashfuddoja, M.; Prasath, R.G.R.; and Ramji, M. (2014). Study on experimental characterization of carbon fiber reinforced polymer panel using digital image correlation: A sensitivity analysis. *Optics and Lasers in Engineering*, 62, 17-30.
26. Simunovic, G.; Svalina, I.; Simunovic, K.; Saric, T.; Havrlisan, S.; and Vukelic, D. (2016). Surface roughness assessing based on digital image features. *Advances in Production Engineering & Management*, 11, 2, 93-104.

27. Lee, B.Y.; and Tarng, Y.S. (2001).Surface roughness inspection by computer vision in turning operations. *International Journal of Machine Tools & Manufacture*, 41, 1251- 1263.
28. Tang, X.; Li, X.; Ding, H.; and Liu, J. (2009). Surface roughness measurement based on image processing and image recognition. *Computers and Simulation in Modern Science*, 91-96.
29. Madhu, S.; and Balasubramanian, M. (2016). Influence of nozzle design and process parameters on surface roughness of CFRP machined by abrasive jet. *Materials and Manufacturing Processes*, 32, 9, 1011-1018.
30. Kumaran, S.T.; Ko, T.J.; Uthayakumar, M.; and Islam, M.M. (2017). Prediction of surface roughness in abrasive water jet machining of CFRP composites using regression analysis. *Journal of Alloys and Compounds*, 724, 1037-1045.
31. Jagadeesh, B.; Dinesh Babu, P.; Nalla Mohamed, M.; and Marimuthu, P (2017). Experimental investigation and optimization of abrasive water jet cutting parameters for the improvement of cut quality in carbon fiber reinforced plastic laminates. *Journal of Industrial Textiles*, 48, 178-200.
32. Xiao, S.; Wang, P.; Gao, H.; and Soulat, D. (2019). A study of abrasive waterjet multi-pass cutting on kerf quality of carbon fiber-reinforced plastics. *International Journal of Advanced Manufacturing Technology*.105, 4527- 4537.
33. Thongkaew, K.; Wang, J.; and Li, M. (2019). An investigation of the hole machining processes on woven Carbon-Fiber Reinforced Polymers (CFRPs) using abrasive waterjets. *Machining Science and Technology*, 23(1), 19-38.
34. Hamza, M.S. (2008). Study the effect of carbon fiber volume fraction and their orientations on the thermal conductivity of the polymer composite materials. *Al-Khwarizmi Engineering Journal*, 4(1), 80-89.
35. Karatas, M.A.; and Gokkaya, H. (2018). A review on machinability of carbon fiber reinforced polymer (CFRP) and glass fiber reinforced polymer (GFRP) composite materials. *Defence Technology* 14, 318-326.
36. Unde, P.D.; Gayakwad, M.D.; and Patil, N.G.; Pawade, R.S.; Thakur, D.G.; and Brahmankar, P.K. (2015). Experimental investigations into abrasive water jet machining of carbon fiber reinforced plastic. *Journal of Composites*, Volume 2015, Article ID 971596,1-9.
37. Dhanawade. A.; Kumar, S.; and Kalmekar, R.V. (2016). Abrasive water jet machining of Carbon Epoxy composite. *Defence Science Journal*, 66(5), 522-528.